PHYSICAL REVIEW D

PARTICLES AND FIELDS

THIRD SERIES, VOLUME 24, NUMBER 9 1 NOVEMBER 1981

Study of the reaction $\pi^- p \to n\Lambda\bar{\Lambda}$ at 6.0 and 7.0 GeV/c

M. J. Stangl,* N. M. Cason, J. M. Bishop, N. N. Biswas, V. P. Kenney, V. A. Polychronakos,† R. C. Ruchti, and W. D. Shephard

University of Notre Dame, Notre Dame, Indiana 46556

J. M. Watson

Argonne National Laboratory, Argonne, Illinois 60439

(Received 10 November 1980)

The $\Lambda\bar{\Lambda}$ system produced in the reaction $\pi^- p \to n\Lambda\bar{\Lambda}$ at 6.0 and 7.0 GeV/c has been studied utilizing the ANL 1.5-m streamer-chamber facility. A 400 000-photograph exposure yielded 284 unweighted $n\Lambda\bar{\Lambda}$ events. The cross section for the reaction is $0.51 \pm 0.22\ \mu$b at 6.0 GeV/c and $1.21 \pm 0.23\ \mu$b at 7.0 GeV/c. No significant indications of baryonium states decaying into $\Lambda\bar{\Lambda}$ are found.

I. INTRODUCTION

We present the analysis of data on the reaction

$$\pi^- p \to n\Lambda\bar{\Lambda} \tag{1}$$

at 6.0 and 7.0 GeV/c. The experiment was performed at the Argonne National Laboratory Zero Gradient Synchrotron (ZGS) utilizing the 1.5-m streamer-chamber facility. The primary purpose of the experiment was to study the $K_S^0 K_S^0$ system produced peripherally in the reaction

$$\pi^- p \to n K_S^0 K_S^0 . \tag{2}$$

A detailed description of the experimental apparatus and analysis of reaction (2) has previously been published.[1]

One motivation for studying the $\Lambda\bar{\Lambda}$ system was to search for baryonium states. If baryonium resonances do indeed exist, the $\Lambda\bar{\Lambda}$ channel would be a particularly interesting place to look for them since it is a pure $I=0$, two-body final state; in addition, it would be possible to get information on the spin-parity of such resonances by observing the Λ and $\bar{\Lambda}$ polarizations through their weak decays.

Because of the low cross sections involved, the bulk of the reported work on the $\Lambda\bar{\Lambda}$ system has been from experiments studying inclusive strange particle production.[2] Only two other experiments have reported results on the $n\Lambda\bar{\Lambda}$ final state.[3,4] Of these, the one most directly comparable to this work is that reported by Beusch *et al.*,[3] with data at 7.0 and 12.0 GeV/c.

II. DATA REDUCTION

The 400 000 streamer-chamber photographs were scanned for all double-vee events which were then measured and processed using the standard bubble-chamber programs TVGP and SQUAW, modified for use with the streamer chamber. For every vee the K_S^0, Λ, $\bar{\Lambda}$, and γ mass hypotheses were tried. For every event with both vees being consistent with originating at a common production vertex point and satisfying at least one mass hypothesis [three-constraint (3C) fit], the following multivertex final-state hypotheses were tried, depending on the nature and number of the vee fits: ΛK_S^0, $\Lambda K_S^0 \pi^0$, $n K_S^0 K_S^0$, and $n\Lambda\bar{\Lambda}$. All the events which failed to obtain a 3C fit for both vees were remeasured and reprocessed.

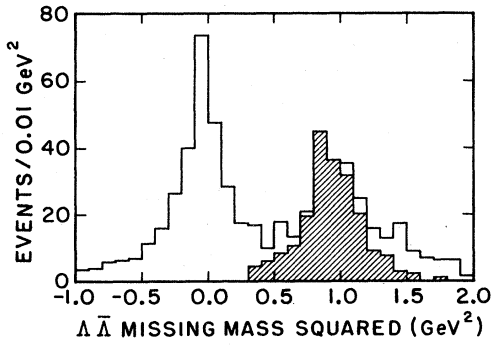

FIG. 1. Distribution of the square of the missing mass recoiling from the $\Lambda\bar{\Lambda}$ system for all $\Lambda\bar{\Lambda}$ candidates. The cross-hatched events are the events in the final data sample.

TABLE I. Corrections and cross sections for the $nK_S^0K_S^0$ state.

Incident momentum (GeV/c)	6.0	7.0
Raw cross section $NA/\rho LN_0$ (μb)[a]	2.42 ± 0.17	2.14 ± 0.14
Nonhydrogen events: F_1	0.74 ± 0.07	0.74 ± 0.07
No fits: F_2	1.05 ± 0.05	1.05 ± 0.05
Neutral decay mode: F_3	2.115	2.115
Average weight: F_4	2.25	2.02
Streamer chamber insensitive: F_5	1.068 ± 0.006	1.101 ± 0.006
Inefficiency of scintillation counters: F_6	1.06 ± 0.04	1.06 ± 0.04
Missing-mass and χ^2 cuts: F_7	0.95 ± 0.02	1.05 ± 0.02
$\sigma(\pi^- p \to nK_S^0K_S^0)$ (μb)[b]	9.64 ± 1.27	8.69 ± 1.13

[a] Calculated with corrected beam track length.
[b] $\sigma = \sigma_{raw}F_1F_2F_3F_4F_5F_6F_7$.

The final sample of 284 $n\Lambda\bar{\Lambda}$ events was selected from the 1244 candidates for which one vee has a 3C-Λ fit and the other a 3C-$\bar{\Lambda}$. In Fig. 1 the missing mass squared (MM^2) spectrum for these 1244 candidates is shown. There is the expected peak present at the mass of the neutron, but there is also a peak near $MM^2 = 0$. These latter events are primarily ΛK_S^0 events, and events fitting the ΛK_S^0 hypothesis were removed from the sample. The MM^2 distribution of events which fit the $n\Lambda\bar{\Lambda}$ hypothesis contains a long tail of events below the neutron peak. For further analysis, the MM^2 was required to be greater than 0.32 GeV^2. In addition, events were required to fit the $n\Lambda\bar{\Lambda}$ multivertex hypothesis with $\chi^2 \leq 20$ (confidence level $\geq 0.5\%$ for the seven-constraint multivertex hypothesis) for further analysis. With these cuts, the final $n\Lambda\bar{\Lambda}$ data sample consists of 46 events at 6.0 GeV/c and 238 events at 7.0 GeV/c. These events are shown cross-hatched in Fig. 1.

Since the experiment contains no γ veto, the possible existence of background due to $n\Sigma^0\bar{\Sigma}^0$, $n\Sigma^0\bar{\Lambda}$, and $n\Lambda\bar{\Sigma}^0$ has been studied using Monte Carlo events. The missing-mass spectrum of Fig. 1 would peak at 1.27 GeV^2 for $\Sigma^0\bar{\Sigma}^0$ events and at 1.05 GeV^2 for the other final states. There is no evidence for significant production of these backgrounds in Fig. 1, and we estimate that they probably contribute less than 10% to our data sample.

A weighting factor was determined for each event and was defined as the inverse of the detection probability for that event. The Monte Carlo method used to determine these factors for the $n\Lambda\bar{\Lambda}$ data sample was similar to that used for the $nK_S^0K_S^0$ sample.[1] The average weight is 2.39 at 7.0 GeV/c and 2.70 at 6.0 GeV/c. The average weights vary slowly as a function of the $\Lambda\bar{\Lambda}$ mass and as a function of t_{pn}, the four-momentum transfer from the proton to the neutron. In the rest of this work shaded histograms indicate unweighted distributions and unshaded histograms weighted distributions.

TABLE II. Corrections and cross sections for the $n\Lambda\bar{\Lambda}$ state.

Incident momentum (GeV/c)	6.0	7.0
T', T	34.55, 1124.28	230.94, 2458.19
T'/T	0.0307 ± 0.0083	0.0939 ± 0.0101
Raw cross section (μb)	0.0744 ± 0.0208	0.201 ± 0.025
Neutral decay mode: F_3'	2.43	2.43
Average weight: F_4'	2.47	2.48
Missing-mass and χ^2 cuts: F_7'	1.30 ± 0.30	1.10 ± 0.10
$\sigma(\pi^- p \to n\Lambda\bar{\Lambda})$ (μb)	0.51 ± 0.22	1.21 ± 0.23
σ for $-t(p \to \Lambda) > 2.0$ (GeV/c)^2 (μb)	0.22 ± 0.11	0.58 ± 0.12

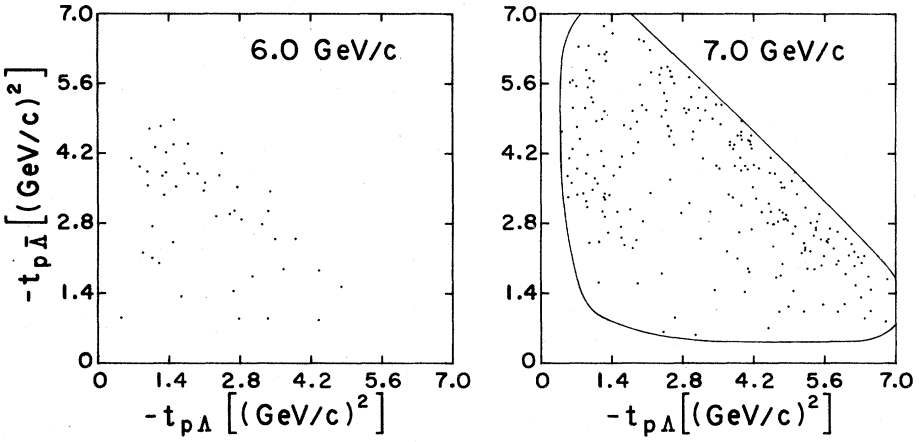

FIG. 2. Scatter plots of $-t_{p\bar{\Lambda}}$ vs $-t_{p\Lambda}$ for the 6.0- and 7.0-GeV/c data separately. The kinematic limit shown on the 7.0-GeV/c data is for a beam momentum of 7.2 GeV/c.

III. THE $n\Lambda\bar{\Lambda}$ CROSS SECTION

The cross section for reaction (1) was found by comparison with that for reaction (2). The latter cross sections were quite consistent with results from other $nK_S^0K_S^0$ experiments. The factors which entered into the measurement of the $nK_S^0K_S^0$ cross sections are summarized in Table I. All of these factors are the same as those for the $n\Lambda\bar{\Lambda}$ final state except for the raw cross section, the neutral decay mode F_3, the average weight F_4, and the missing-mass and χ^2 cuts F_7.

The raw cross section for $n\Lambda\bar{\Lambda}$ can be determined by the relation

$$\sigma_{\mathrm{raw}}(\pi^- p \to n\Lambda\bar{\Lambda}) = \sigma_{\mathrm{raw}}(\pi^- p \to nK_S^0K_S^0) \times (T'/T),$$

where T' and T are the reconstructed numbers of true events of the $n\Lambda\bar{\Lambda}$ and $nK_S^0K_S^0$ types, respectively, in a given data sample. The factor F_3 is obtained from the inverse of the probability that either or both K^0's decay into two neutral pions. A similar factor F_3' can be calculated to account for the neutral decay mode of the Λ and $\bar{\Lambda}$, and is 2.43. Given the average weights for the $n\Lambda\bar{\Lambda}$ events, F_4', and the correction factor for the cuts, F_7', one can then calculate the cross section as follows:

$$\sigma(\pi^- p \to n\Lambda\bar{\Lambda}) = \sigma_{\mathrm{raw}}(\pi^- p \to n\Lambda\bar{\Lambda}) \times F_1F_2F_3'F_4'F_5F_6F_7'.$$

(Note that F_4' is somewhat different from the average weight for the complete sample becuase of more restrictive cuts being applied for the cross-section data.)

The cross sections for $\pi^- p \to n\Lambda\bar{\Lambda}$ at 6.0 and 7.0 GeV/c are presented in Table II, along with the appropriate correction factors. The value at 7.0 GeV/c can be compared to that obtained by

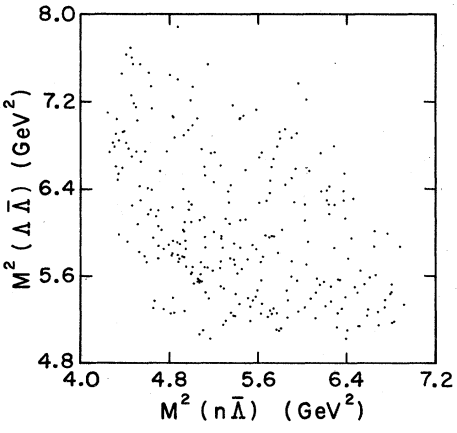

FIG. 3. Scatter plot of the $\Lambda\bar{\Lambda}$ effective mass squared vs the $n\bar{\Lambda}$ effective mass squared.

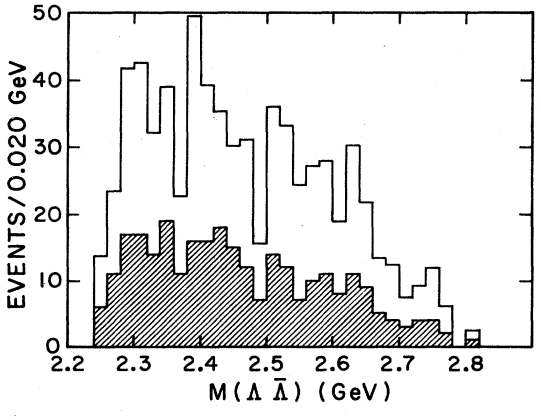

FIG. 4. Distribution of the $\Lambda\bar{\Lambda}$ effective mass for the $n\Lambda\bar{\Lambda}$ events. The cross-hatched histogram is the unweighted data and the full histogram is the weighted data.

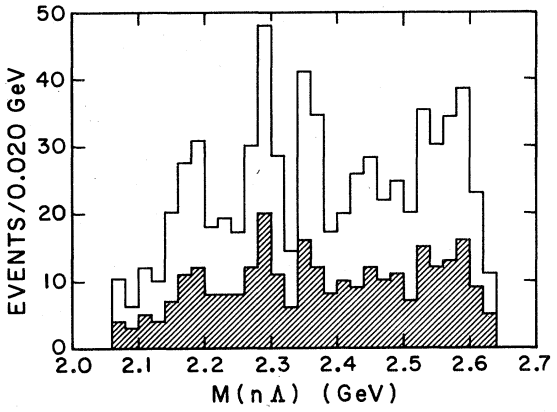

FIG. 5. Distribution of the $n\Lambda$ effective mass for the $n\Lambda\bar{\Lambda}$ events. The cross-hatched histogram is the unweighted data and the full histogram is the weighted data.

Beusch *et al.*[3] They observed 24 events at 7.0 GeV/c which translated into 195 weighted events and a cross section of 0.27 ± 0.07 μb. This is approximately four times smaller than the result given in Table II.

It is possible that there may be systematic uncertainties for events in the region of low $-t_{p\Lambda}$. These errors could arise from a combination of low statistics and poor acceptance for slow Λ's. However, this is not a problem for the region $-t_{p\Lambda} > 2.0$ (GeV/c)^2. Consequently, the cross sections are given separately in Table II for $-t_{p\Lambda} > 2.0$ (GeV/c)^2.

IV. ANALYSIS OF THE $n\Lambda\bar{\Lambda}$ FINAL STATE

Scatter plots of $-t_{p\bar{\Lambda}}$ versus $-t_{p\Lambda}$ are shown in Fig. 2 for the 6.0- and 7.0-GeV/c data separately. The third invariant momentum transfer, $-t_{p\Lambda}$, is proportional to the distance from the base of the

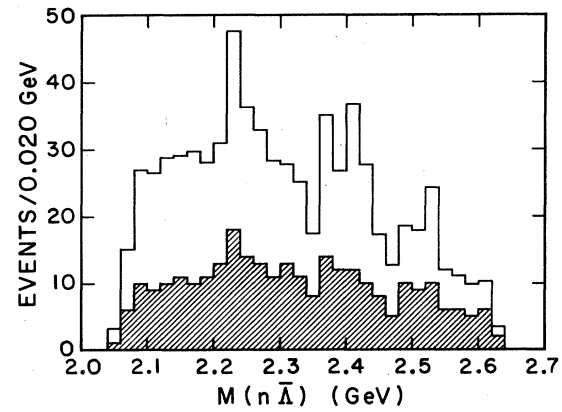

FIG. 6. Distribution of the $n\bar{\Lambda}$ effective mass for the $n\Lambda\bar{\Lambda}$ events. The cross-hatched histogram is the unweighted data and the full histogram is the weighted data.

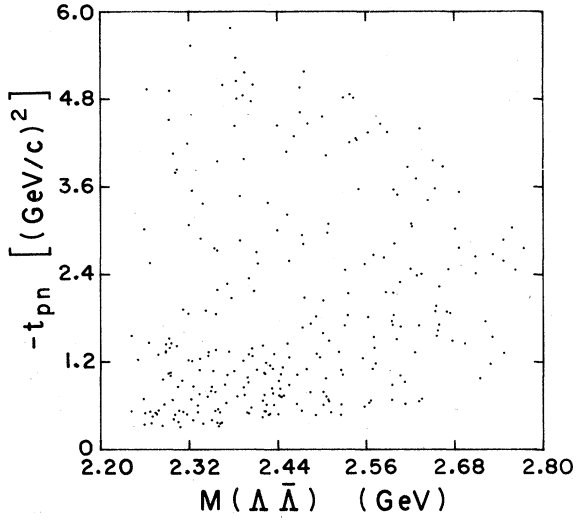

FIG. 7. Scatter plot of $-t_{pn}$ vs the $\Lambda\bar{\Lambda}$ effective mass.

"triangle." There is obvious clustering of events at maximum $|-t_{p\Lambda} - t_{p\bar{\Lambda}}|$ or low $|-t_{pn}|$. In addition, a subset of events with low $|-t_{p\Lambda}|$ is also present. In both cases, however "low" $|t|$ goes somewhat above 1.0 (GeV/c)^2.

A scatter plot of the $\Lambda\bar{\Lambda}$ effective mass squared as a function of the $\bar{\Lambda}n$ effective mass squared is given in Fig. 3. The distribution of events is fairly uniform, although there may be some clustering in the region corresponding to low mass for both combinations. The distributions of the $\Lambda\bar{\Lambda}$, Λn, and $\bar{\Lambda}n$ effective masses are shown in Figs. 4, 5, and 6, respectively. These effective-mass distributions contain no statistically significant enhancements.

The scatter plot of $-t_{pn}$ vs the $\Lambda\bar{\Lambda}$ effective

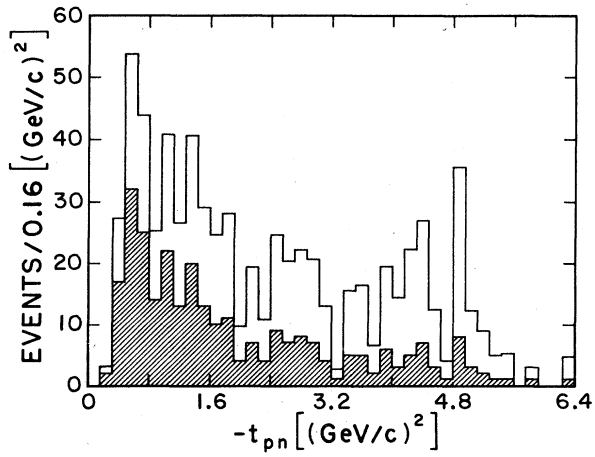

FIG. 8. Distribution of $-t_{pn}$ for the $n\Lambda\bar{\Lambda}$ events. The cross-hatched histogram is the unweighted data and the full histogram is the weighted data.

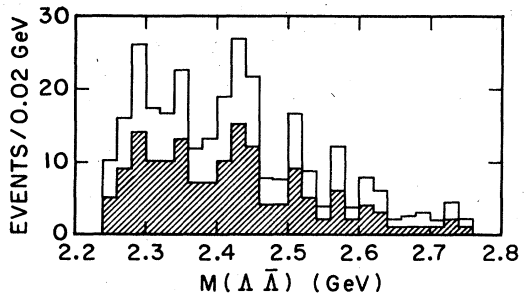

FIG. 9. Distribution of the $\Lambda\bar{\Lambda}$ effective mass for those events with $-t_{pn} < 1.6$ (GeV/c)^2. The cross-hatched histogram is the unweighted data and the full histogram is the weighted data.

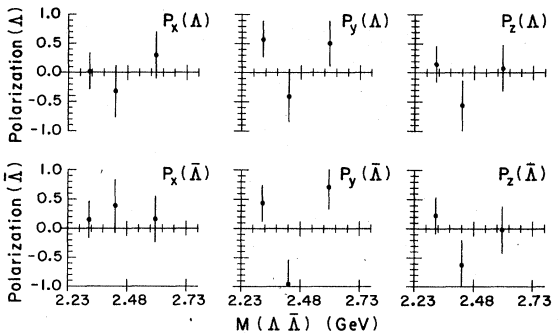

FIG. 10. Polarizations of the Λ and $\bar{\Lambda}$ as a function of the $\Lambda\bar{\Lambda}$ effective mass. The components Px, Py, and Pz are defined in a coordinate system in the $\Lambda\bar{\Lambda}$ rest frame (see text).

mass for the combined data is shown in Fig. 7. There is a band of events of greater density below a $|t_{pn}|$ value of about 1.6 (GeV/c)^2 which is evident in the projected t_{pn} distribution of Fig. 8. The data sample used in further analysis consists of the events in this band, i.e., $|t_{pn}| \leq 1.6$ (GeV/c)^2.

The $\Lambda\bar{\Lambda}$ effective-mass distribution for these events is shown in Fig. 9. The only suggestion of an enhancement is in the region from 2400 to 2460 MeV/c^2. This is, however, only a 2.5-standard-deviation effect. (The $\Lambda\bar{\Lambda}$ effective-mass resolution is about 10 MeV and, therefore, if the enhancement is real, its true width is of the order of 40 MeV.)

In order to study other aspects of the data in light of the possible structure in the $\Lambda\bar{\Lambda}$ effective-mass distribution, the sample was divided into three $\Lambda\bar{\Lambda}$ mass bins, one which contained the enhancement from 2.40 to 2.46 GeV and the other two corresponding to the mass regions below and above this central bin. The Λ and $\bar{\Lambda}$ polarizations, the $\Lambda\bar{\Lambda}$ decay angular distributions, and the t_{pn} distribution were studied separately for each of the three mass bins.

The polarizations were calculated for two different coordinate systems. The first is defined in the laboratory frame and has its z axis perpendicular to the production plane, i.e., the plane formed by the beam and the Λ ($\bar{\Lambda}$). The y axis is in the direction of the beam. In this system parity conservation in production requires that the y component of the polarization of the Λ ($\bar{\Lambda}$) should be zero. In the second coordinate system the z axis is normal to the ($\pi^-\Lambda\bar{\Lambda}$) plane in the $\Lambda\bar{\Lambda}$ rest frame, and the y axis is in the direction of the Λ. This frame would be sensitive to polarization effects for a peripherally produced resonance which decays into a $\Lambda\bar{\Lambda}$ system.

The y and z components of the Λ ($\bar{\Lambda}$) polarization as calculated in the first system (not shown) are

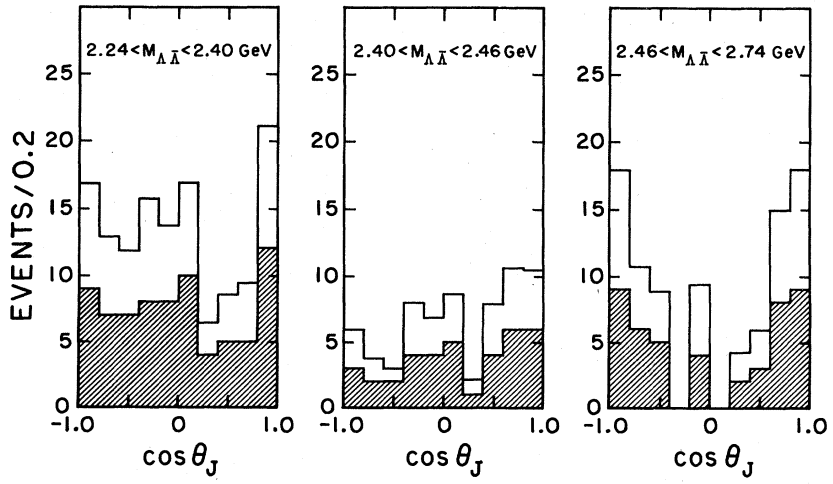

FIG. 11. Distribution of cos θ_J, the t-channel decay angle of the $\Lambda\bar{\Lambda}$ system. The cross-hatched histogram is the unweighted data and the full histogram is the weighted data.

consistent with being equal to zero for all mass bins. The polarizations calculated in the second system are shown in Fig. 10. The x components are consistent with zero, while both the y and z components are somewhat positive in the first bin, go negative in the central region, and return to the axis or above in the high-mass bin. Thus, just as with the mass distribution, there is a hint of changed behavior in the mass region about 2.43 GeV/c^2, but of marginal statistical significance.

The distributions of the cosine of the Jackson decay angle (t channel) in the three mass regions are shown in Fig. 11. There is no evidence for unusual behavior in the 2.43-GeV/c^2 mass region in these distributions. Similarly the t_{pn} distributions (not shown) do not provide evidence for a rapid change in the 2.43-GeV/c^2 mass range.

To conclude, we find no statistically significant evidence for baryonium states decaying into $\Lambda\bar{\Lambda}$ in our data. Even though this experiment contains an order of magnitude more data than previous experiments, it is clear that another order of magnitude in statistics would be necessary to draw definitive conclusions in this regard.

ACKNOWLEDGMENTS

It is a pleasure to thank the streamer-chamber personnel, the ZGS staff, and the Notre Dame scanning staff for their dedicated efforts. We also acknowledge the invaluable assistance of R. Erichsen, W. Rickhoff, and A. Horvath. This research was supported in part by The National Science Foundation, Grant No. PHY78-06722, and by the Department of Energy.

---

*Present address: Bell Laboratories, Naperville, Illinois.

†Present address: Brookhaven National Laboratory, Upton, New York.

[1]V. A. Polychronakos *et al.*, Phys. Rev. D 19, 1317 (1979).

[2]C. Baltay *et al.*, Phys. Rev. 140B, 1027 (1965); D. Bertrand *et al.*, Nucl. Phys. B128, 365 (1977); P. Bosetti *et al.*, *ibid.* B94, 21 (1975); C. Y. Chien *et al.*, Phys. Rev. 152, 1171 (1966); G. P. Fisher *et al.*, *ibid.* 161, 1335 (1967); B. R. French, J. Moebes, and C. Pols, Nucl. Phys. B119, 237 (1977); S. Lichtman *et al.*, *ibid.* B105, 229 (1976); B. Musgrave *et al.*, Nuovo Cimento 35, 735 (1965); R. Raja *et al.*, Phys. Rev. D 15, 627 (1977).

[3]W. Beusch *et al.*, Phys. Lett. 28B, 211 (1968).

[4]B. P. Barkov *et al.*, Yad. Fiz. 22, 223 (1975) [Sov. J. Nucl. Phys. 22, 113 (1976)].